Journal of Organometallic Chemistry, 333 (1987) 85–95
Elsevier Sequoia S.A., Lausanne – Printed in The Netherlands

Reaction of tetracyanoethene with tricarbonyliron complexes of some substituted 7-methylenecycloheptatrienes and the subsequent isomerization of the initial addition products

Desmond Cunningham, Noel Hallinan, Grainne Moran and Patrick McArdle*
Chemistry Department, University College Galway (Ireland)

(Received March 19th, 1987)

Abstract

An NMR study of tetracyanoethene (tcne) addition to substituted (η^4-7-methylenecycloheptatriene)Fe(CO)$_3$ complexes shows that 1,3-addition is the dominant initial reaction. Subsequent isomerisation of these 1,3-adducts to 1,6- or 1,8-adducts is controlled by steric factors. Frontier orbital analyses allow concerted pathways to be identified for each observed addition and isomerisation. The crystal structure of the tcne adduct of (η^4-7-phenylmethylenecycloheptatriene)Fe(CO)$_3$ establishes an *exo* geometry for the phenyl substituent.

Introduction

Previous studies on the reaction of tetracyanoethene (tcne) with (η^4-7-methylenecycloheptatriene)Fe(CO)$_3$ complexes have been confined to kinetic measurements of the rate of addition and to examination of reactions by low-field NMR [1]. It was decided to attempt the monitoring of these reactions by high field NMR spectroscopy and to determine the geometry of one of the 1,8-adducts by determination of its crystal structure.

Reactions with tcne

(η^4-7-Phenylmethylenecycloheptatriene)Fe(CO)$_3$ (1a)

Complex **1a** was reacted with one equivalent of tcne in acetone-d_6 and the reaction was followed by ^{1}H NMR. The two singlets assigned to H(7) in *cis*- and *trans*-**1a** (Scheme 1) at 7.00 and 6.70 ppm, were on addition of tcne immediately replaced by two signals at lower field, 7.36 and 7.18 ppm. The resonance at 7.18 ppm disappeared in 8 min with concurrent growth of a narrow triplet at 5.22 ppm. The singlet at 7.36 ppm disappeared more slowly, over 3 h, and a singlet at 6.82 ppm increased in intensity reaching a maximum at 90 min. As the signals at 7.36

0022-328X/87/$03.50

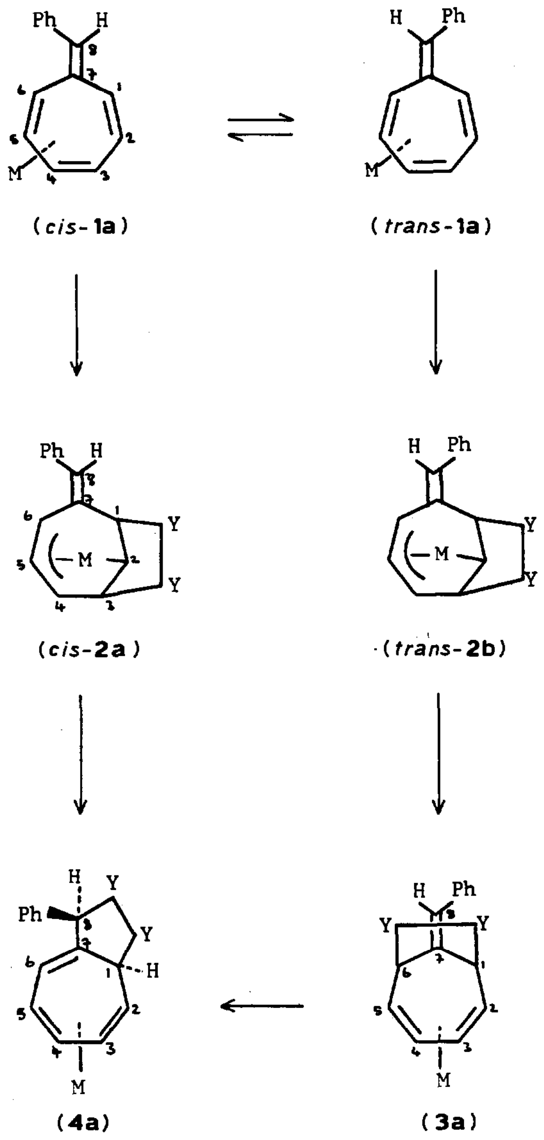

Scheme 1. M = Fe(CO)$_3$; Y = (CN)$_2$.

and 6.82 disappeared the resonance at 5.22 ppm continued to increase. After 11 h a spectrum of only one isomeric adduct was observed. This final product has been previously assigned the 1,8-structure (**4a**).

The resonances at 7.36 and 7.18 ppm and other resonances in the spectrum can be interpreted as being due to *cis*- and *trans*-**2b** respectively, resulting from relatively rapid 1,3-addition of tcne to the uncoordinated side of *cis*- and *trans*-**1b** (Scheme 1). The characteristic high-field resonances expected for protons attached to the Fe–C σ bond are observed at 2.36 and 1.90 ppm. One of these isomers (reasonably presumed to be *cis*-**2a**) is transformed directly to the 1,8-adduct **4a**.

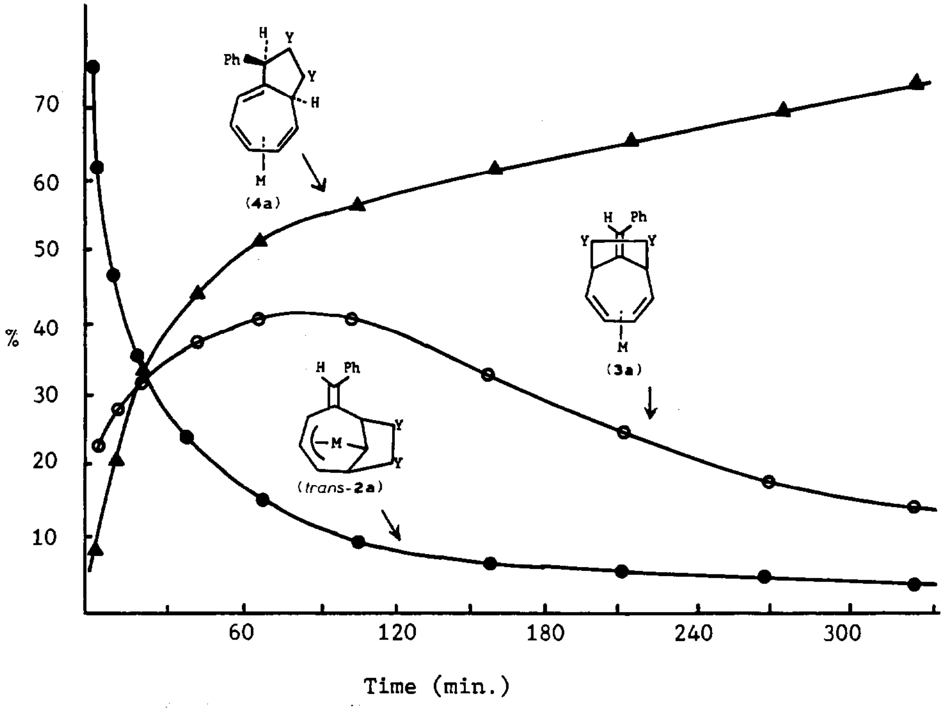

Fig. 1. Time profile of the reaction of tcne with **1a**.

Trans-**2a** does not undergo this direct 1,3- to 1,8-isomerisation. The growth and decay of a singlet at 6.82 ppm provides evidence for another transient isomer. The structure of this isomer was deduced from spin decoupling experiments and by spectral subtraction. The new intermediate is assigned the 1,6-structure **3a**. A time profile plot of the species which may be followed with reasonable accuracy is given in Fig. 1. The crystal structure of the final product is described below. This structure clearly establishes that the phenyl group is *exo* with respect to iron. The observation of the 1,6-intermediate allows a simple explanation for the observation of only one final 1,8-isomer. *Cis*-**2a** readily isomerises to *exo*-**4a**. The new C–C bond forming on the side of the molecule away from the bulky phenyl group. *Trans*-**2a** would on isomerisation to *endo*-**4a** require the formation of the new C–C bond on the same side as the phenyl group. Isomerisation of *trans*-**2a** to the 1,6-isomer provides an alternative path to *exo*-**4a** which again allows formation of the new C–C bond on the side away from the phenyl group and permits an *exo* geometry to develop for **4a**. If indeed it is impossible to form a new C–C bond on the same side as a phenyl group then the diphenyl complex **1b** should not give any 1,8-adduct.

*(η^4-7-Diphenylmethylenecycloheptatriene)Fe(CO)$_3$ (**1b**)*

Addition of tcne, one equivalent, to **1b** in acetone-d_6 solution resulted in the immediate formation of a 1,3-adduct (**2b**). This adduct slowly isomerises to an equilibrium concentration of the 1,6-adduct (**3b**). After 48 h the ratio of **2b** to **3b** was close to 1/1 and no further change with time was observed. This clearly

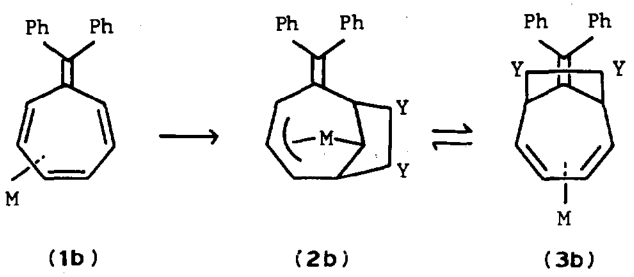

Scheme 2

demonstrates that when isomerisation to the 1,8-adduct is precluded, 1,3- to 1,6-isomerisation takes place (Scheme 2).

(η^4-7-Methylmethylenecycloheptatriene)Fe(CO)$_3$ (1c)

This complex has been reported to react with tcne to give two 1,8-isomers in a 1/3 ratio [2]. The progress of this reaction was monitored by observing the doublet resonances of the methyl groups. The complexity of the 3–7 ppm region during the reaction did not permit the assignment of the ring protons of the intermediate compounds. On addition of tcne, one equivalent, to **1c** in acetone-d_6 the pair of methyl doublets due to *cis*- and *trans*-**1c** at 1.76 and 1.84 ppm were after 4 min replaced by a pair of doublets at lower field, 2.05 and 2.12 ppm, and a pair at higher field at 1.53 and 1.67 ppm. The latter pair are due to the isolated 1,8-adducts (**4c**). In a spectrum taken after 10 min an extra single doublet is observed at 1.97 ppm. After 40 min this resonance at 1.97 ppm had increased with an accompanying decrease in the doublet pair at 2.05 and 2.12 ppm and surprisingly in the resonance at 1.67 ppm. After 3 h the only methyl resonances observed were those at 1.53 and 1.67 ppm due to **4c** and a very weak doublet at 1.97 ppm. Throughout the reaction the integration of the residual proton peak of the acetone-d_6 solvent relative to all

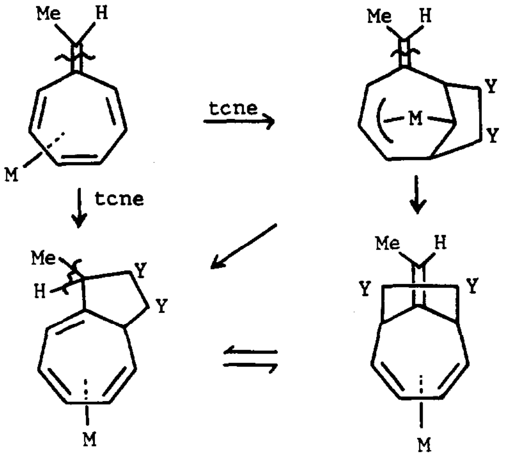

Scheme 3

of the methyl resonances showed that the observed changes were due to isomerisation among the observed species. The unassigned resonances, the pair of doublets at 2.05 and 2.12 ppm and the doublet at 1.97 ppm are assigned to the isomers of **2c** and to **3c**. Since *cis* and *trans* isomers are not possible for **3c** it is the only reasonable structure which could give rise to a single methyl doublet. The assignment of the **2c** methyl resonances is less certain but by analogy with the phenyl derivatives it is likely that 1,3-adducts would be present early in the reaction. Since the first spectrum obtained after tcne addition contained peaks due to the 1,8-adduct, both 1,3- and 1,8-addition may have occurred in this case. The observed reactions are illustrated in Scheme 3.

Extended Hückel Calculations

tcne addition

The atomic charges and HOMO coefficients calculated for (η^4-7-methylenecycloheptatriene)Fe(CO)$_3$ are given in Table 1. The charge distributions within the seven-membered ring are similar to those found for other η^4-triene complexes [3], with C(1), C(3) and C(6) bearing negative charges. In addition the 8-position carries a negative charge. On the basis of charge alone electrophilic tcne addition could involve any two of these positions.

Since the LUMO of tcne is unsymmetrical frontier orbital theory would suggest, on the basis of the calculated coefficients in Table 1, that 1,3-, 1,4- and 1,8-addition are all symmetry allowed. Thus the observed modes of addition are symmetry allowed. No experimental evidence has been found for 1,4-addition for **1a**, **1b** or **1c**.

Isomerization of initially observed adducts

The isomerisation of initially formed 1,3-adducts to 1,5-, 1,6- and 1,8-adducts have all been observed. A frontier orbital analysis of these isomerisations has been made [4] and separate analyses of 1,3- to 1,5- and 1,3- to 1,6-isomerisations have been made [5,6]. It was therefore of interest to see if the new isomerisations reported here could be provided with a concerted pathway.

The 1,6- to 1,8-mode of isomerisation has not been examined previously. This reaction is essentially a (1,3)-sigmatropic carbon migration, with the metal remaining η^4-bonded to C(2)–C(5) of the ring throughout the reaction (Fig. 2). It therefore corresponds to the sigmatropic rearrangement of a substituted methylene cyclopentane. The Woodward–Hoffman rules [7] predict that a (1,3)-suprafacial migration, with inversion at the migrating carbon, is symmetry-allowed and could therefore be concerted. However, experimental studies of (1,3)-shifts [8] in systems such as 1,3-dimethylenecyclopentane suggest that the mechanisms involve the formation of

Table 1

Atomic charges and HOMO coefficients

	C_1	C_2	C_3	C_4	C_5	C_6	C_7	C_8
Charges	−0.023	−0.016	−0.013	0.013	0.010	−0.017	−0.010	−0.040
Coefficients	0.343	0.334	−0.336	−0.233	0.170	0.228	−0.233	−0.492

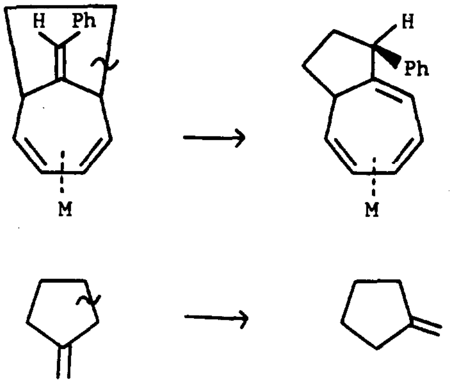

Fig. 2. 1,6–1,8 Isomerisation.

biradical intermediates. This reaction has been examined in the cavity of an ESR spectrometer and no ESR signals were observed.

A 1,3- to 1,6-isomerisation has been previously studied in the case of the tcne adduct of (η^4-cycloheptatriene)Fe(CO)$_3$ [6] where it was concluded that the reaction

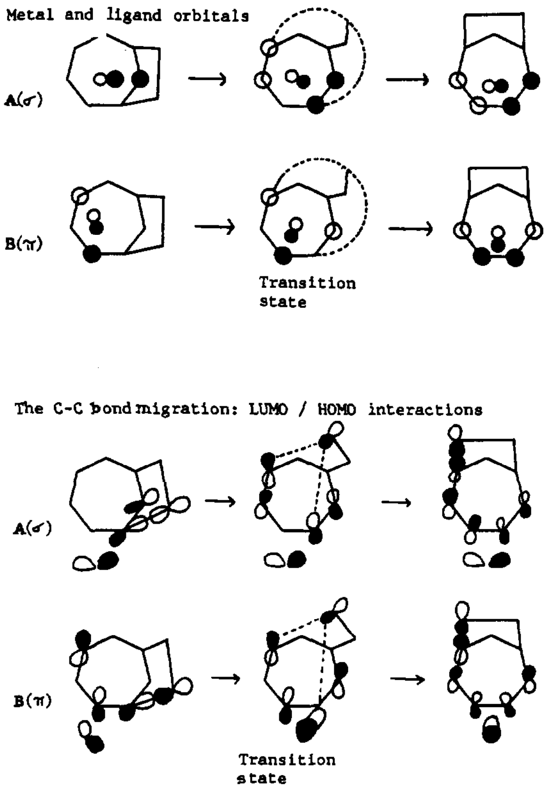

Fig. 3. Frontier orbital correlations for 1,3–1,6 isomerisation.

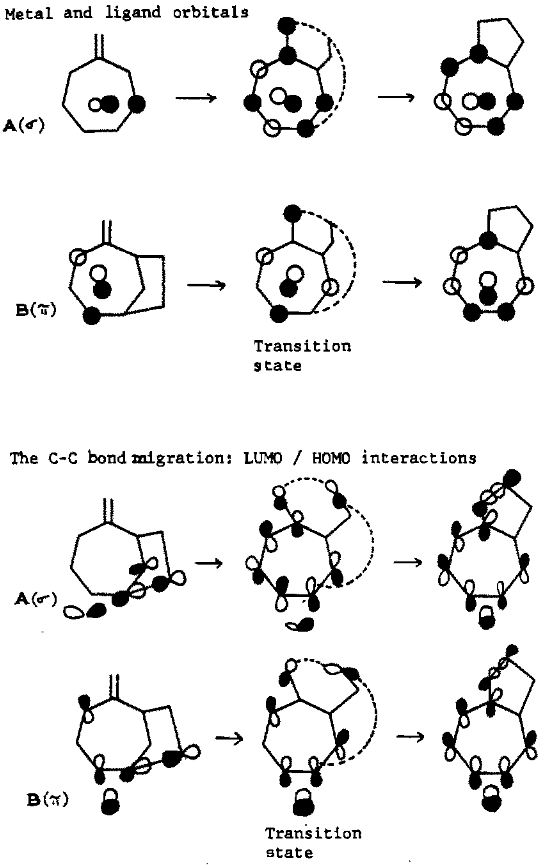

Fig. 4. Frontier orbital correlations for 1,3–1,8 isomerisation.

could follow a concerted pathway. The present results are similar and the two highest occupied molecular orbitals, **A** and **B**, are shown schematically in Fig. 3. The molecular orbitals for the proposed transition state resemble those of (η^5-pentadienyl)Fe(CO)$_3$ [9]. The product is an η^4-diene complex [10]. The σ- and π-bonding frontier orbitals in the 1,3-adduct can be seen to transform into the two principle (η^4-diene)Fe(CO)$_3$ bonding orbitals in the 1,6-product.

The analysis of the frontier orbitals for the 1,3- to 1,8-mode of isomerisation is illustrated in Fig. 4. The transition state in this case resembles an (η^5-heptatrienyl)Fe(CO)$_3$ complex and the 1,8-product is a derivative of (η^4-cycloheptatriene)Fe(CO)$_3$, whose orbitals have been reported [3,11]. It is clear that the symmetry requirements of the carbon migration in this case are the reverse of those discussed for the 1,3- to 1,6-migration. Again the frontier orbital approach allows possible concerted pathways to be identified for each of the isomerisation reactions.

Crystal structure of 4a

The crystal structure of **4a** was determined to confirm the geometry about C(8). The structure is illustrated in Fig. 5 and the phenyl substituent is clearly *exo* with

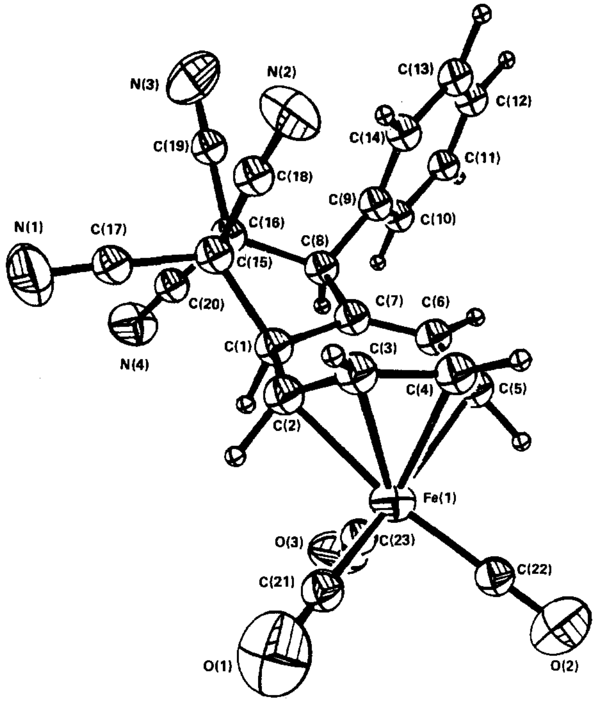

Fig. 5. ORTEP drawing 12 of the crystal structure of **4a**.

respect to the iron atom. This is exactly the geometry which results from 1,3- to 1,8-isomerisation of *cis*-**2b**.

The crystal data are given in Table 2 and the atomic coordinates, bond lengths, and bond angles in Tables 3, 4 and 5. The structure was solved by direct methods and refined by full matrix least-squares using SHELX76 [13]. The iron, oxygen and nitrogen atoms were refined anisotropically. All other non-hydrogen atoms were refined isotropically. Hydrogen atoms were included at calculated positions. Tables

Table 2

Crystal data for $C_{23}H_{12}N_4O_3Fe$ (**4a**)

Monoclinic space group $P2_1/a$

Unit cell a 12.824(5), b 13.580(2), c 12.852(3) Å, α 90, β 112.12(2), γ 90 °,

U 2073.46 Å^3, $F(000) = 911.96$, μ 19.59 cm^{-1}, $Z = 4$.

Radiation used	Mo-K_α, λ 0.71069 Å.
Observed reflections	1322 $I > 3\sigma I$.
Parameters	168
Final difference E Map	Max. peak 0.17 e/Å^3 Min. peak −0.14 e/Å^3
Final least-squares cycle	Max. shift/esd < 0.002
Residuals	R 4.82% $R_w = 5.96\%$

Table 3

Atomic coordinates for $C_{23}H_{12}N_4O_3Fe$ (**4a**)

Atom	x	y	z	U_{iso} or U_{eq} *
Fe(1)	−0.07514(8)	−0.11201(7)	0.72896(8)	0.0444(8)*
O(1)	−0.0526(5)	−0.3031(5)	0.8441(5)	0.107(5)*
O(2)	−0.3034(5)	−0.1679(4)	0.5839(5)	0.090(4)*
O(3)	−0.1278(5)	0.0160(4)	0.8852(4)	0.096(4)*
N(1)	0.3953(6)	−0.0518(5)	1.0343(5)	0.089(5)*
N(2)	0.3041(6)	0.0100(5)	0.6867(5)	0.080(5)*
N(3)	0.4300(6)	0.2540(5)	0.8703(6)	0.088(5)*
N(4)	0.2703(5)	0.1888(4)	1.0915(5)	0.072(4)*
C(1)	0.1310(5)	0.0219(4)	0.8368(5)	0.042(2)
C(2)	0.0980(5)	−0.0826(5)	0.8047(5)	0.054(2)
C(3)	0.0690(6)	−0.1272(5)	0.6961(6)	0.066(2)
C(4)	−0.0160(6)	−0.0863(5)	0.6054(6)	0.060(2)
C(5)	−0.0715(6)	0.0014(5)	0.6154(5)	0.051(2)
C(6)	−0.0125(5)	0.0942(5)	0.6643(5)	0.047(2)
C(7)	0.0762(5)	0.1037(4)	0.7566(5)	0.041(2)
C(8)	0.1387(5)	0.1983(4)	0.8006(4)	0.042(2)
C(9)	0.1402(5)	0.2738(4)	0.7153(4)	0.041(2)
C(10)	0.0951(6)	0.3659(5)	0.7179(6)	0.057(2)
C(11)	0.0925(6)	0.4362(6)	0.6382(6)	0.069(2)
C(12)	0.1345(6)	0.4179(6)	0.5591(6)	0.066(2)
C(13)	0.1795(6)	0.3265(5)	0.5544(6)	0.061(2)
C(14)	0.1836(5)	0.2542(5)	0.6334(5)	0.049(2)
C(15)	0.2577(5)	0.0467(4)	0.8634(4)	0.040(2)
C(16)	0.2587(5)	0.1614(5)	0.8861(5)	0.042(2)
C(17)	0.3365(6)	−0.0093(5)	0.9601(6)	0.057(2)
C(18)	0.2868(5)	0.0273(5)	0.7648(5)	0.048(2)
C(19)	0.3548(6)	0.2123(5)	0.8759(5)	0.053(2)
C(20)	0.2669(5)	0.1764(5)	1.0022(6)	0.049(2)
C(21)	−0.0604(7)	−0.2284(7)	0.8000(7)	0.073(2)
C(22)	−0.2135(8)	−0.1449(6)	0.6410(7)	0.068(2)
C(23)	−0.1102(6)	−0.0355(6)	0.8234(6)	0.060(2)

Table 4

Bond lengths (Å) for $C_{23}H_{12}N_4O_3Fe$ (**4a**)

Fe(1)–C(2)	2.100(7)	Fe(1)–C(3)	2.056(8)
Fe(1)–C(4)	2.031(7)	Fe(1)–C(5)	2.134(6)
Fe(1)–C(21)	1.799(10)	Fe(1)–C(22)	1.765(10)
Fe(1)–C(23)	1.779(8)	O(1)–C(21)	1.148(9)
O(2)–C(22)	1.153(9)	O(3)–C(23)	1.143(8)
N(1)–C(17)	1.126(8)	N(2)–C(18)	1.132(8)
N(3)–C(19)	1.144(8)	N(4)–C(20)	1.144(8)
C(1)–C(2)	1.494(9)	C(1)–C(7)	1.497(8)
C(1)–C(15)	1.566(9)	C(2)–C(3)	1.437(10)
C(3)–C(4)	1.378(10)	C(4)–C(5)	1.417(9)
C(5)–C(6)	1.483(9)	C(6)–C(7)	1.305(8)
C(7)–C(8)	1.507(8)	C(8)–C(9)	1.508(8)
C(8)–C(16)	1.598(8)	C(9)–C(10)	1.383(9)
C(9)–C(14)	1.388(8)	C(10)–C(11)	1.391(10)
C(11)–C(12)	1.341(10)	C(12)–C(13)	1.380(10)
C(13)–C(14)	1.399(9)	C(15)–C(16)	1.585(9)
C(15)–C(17)	1.482(10)	C(15)–C(18)	1.473(9)
C(16)–C(19)	1.461(10)	C(16)–C(20)	1.470(10)

Table 5

Bond angles (°) for $C_{23}H_{12}N_4O_3Fe$ (**4a**)

C(3)–Fe(1)–C(2)	40.4(3)	C(4)–Fe(1)–C(2)	71.9(3)
C(4)–Fe(1)–C(3)	39.4(3)	C(5)–Fe(1)–C(2)	83.6(3)
C(5)–Fe(1)–C(3)	71.3(3)	C(5)–Fe(1)–C(4)	39.7(3)
C(21)–Fe(1)–C(2)	92.4(3)	C(21)–Fe(1)–C(3)	94.9(3)
C(21)–Fe(1)–C(4)	123.3(3)	C(21)–Fe(1)–C(5)	162.9(3)
C(22)–Fe(1)–C(2)	167.8(3)	C(22)–Fe(1)–C(3)	127.4(3)
C(22)–Fe(1)–C(4)	97.1(3)	C(22)–Fe(1)–C(5)	91.1(3)
C(22)–Fe(1)–C(21)	89.5(4)	C(23)–Fe(1)–C(2)	93.9(3)
C(23)–Fe(1)–C(3)	132.6(3)	C(23)–Fe(1)–C(4)	134.2(3)
C(23)–Fe(1)–C(5)	97.0(3)	C(23)–Fe(1)–C(21)	99.9(3)
C(23)–Fe(1)–C(22)	97.7(3)	C(7)–C(1)–C(2)	120.3(5)
C(15)–C(1)–C(2)	115.3(5)	C(15)–C(1)–C(7)	99.8(5)
C(1)–C(2)–Fe(1)	116.7(4)	C(3)–C(2)–Fe(1)	68.2(4)
C(3)–C(2)–C(1)	127.6(6)	C(2)–C(3)–Fe(1)	71.4(4)
C(4)–C(3)–Fe(1)	69.3(5)	C(4)–C(3)–C(2)	119.0(7)
C(3)–C(4)–Fe(1)	71.3(4)	C(5)–C(4)–Fe(1)	74.1(4)
C(5)–C(4)–C(3)	121.8(7)	C(4)–C(5)–Fe(1)	66.2(4)
C(6)–C(5)–Fe(1)	117.6(4)	C(6)–C(5)–C(4)	124.0(6)
C(7)–C(6)–C(5)	126.9(6)	C(6)–C(7)–C(1)	125.1(6)
C(8)–C(7)–C(1)	109.2(5)	C(8)–C(7)–C(6)	125.7(5)
C(9)–C(8)–C(7)	117.3(5)	C(16)–C(8)–C(7)	103.2(5)
C(16)–C(8)–C(9)	116.1(5)	C(10)–C(9)–C(8)	118.4(5)
C(14)–C(9)–C(8)	122.7(6)	C(14)–C(9)–C(10)	118.9(6)
C(11)–C(10)–C(9)	119.7(7)	C(12)–C(11)–C(10)	121.7(8)
C(13)–C(12)–C(11)	119.6(7)	C(14)–C(13)–C(12)	120.1(7)
C(13)–C(14)–C(9)	119.9(6)	C(16)–C(15)–C(1)	100.8(4)
C(17)–C(15)–C(1)	113.4(5)	C(17)–C(15)–C(16)	113.2(5)
C(18)–C(15)–C(1)	110.6(5)	C(18)–C(15)–C(16)	110.3(5)
C(18)–C(15)–C(17)	108.5(5)	C(15)–C(16)–C(8)	104.1(4)
C(19)–C(16)–C(8)	114.7(5)	C(19)–C(16)–C(15)	113.4(5)
C(20)–C(16)–C(8)	109.7(5)	C(20)–C(16)–C(15)	108.4(5)
C(20)–C(16)–C(19)	106.5(5)	C(15)–C(17)–N(1)	179.1(8)
C(15)–C(18)–N(2)	176.5(7)	C(16)–C(19)–N(3)	178.0(8)
C(16)–C(20)–N(4)	178.1(7)	O(1)–C(21)–Fe(1)	179.0(7)
O(2)–C(22)–Fe(1)	178.9(7)	O(3)–C(23)–Fe(1)	176.6(7)

of thermal parameters and lists of observed and calculated structure factors are available from the authors.

Within the seven-membered ring the shortest bond is the uncoordinated olefinic bond, C(6)–C(7). The coordinated diene unit shows significant bond alternation typical of a complex with excited state geometry for the coordinated diene. C(3)–C(4) is significantly shorter than both C(2)–C(3) and C(4)–C(5). There are no significant differences in bond lengths within the carbonyl groups. The largest deviation from linearity, (3.4°) is shown by Fe–C(23)–O(3). While the the C–C and C–N distances involving the cyano groups are very similar, the CN pair on C(16) show longer C–N distances. There are no large deviations from linearity and the largest 3.5° is shown by C(15)–C(18)–N(2).

The five-membered ring is not planar, C(15) being 0.46 Å from the best plane through the five atoms. The coordinated diene unit, which is approximately planar, and the uncoordinated portion of the cycloheptatriene ring are folded with an angle of 41°. This fold angle is typical and close to that reported for (7-phenylcycloheptatriene)Fe(CO)$_3$ [14].

Experimental

Extended Hückel Calculations were carried out using a model geometry derived from that of (η^4-tropone)Fe(CO)$_3$ [15] and the Forticon program [16]. Further details of the calculations are given in reference [3]. NMR spectra were obtained on a JEOL GX-270 spectrometer. The crystal data were collected on a Hilger and Watts Y290 diffractometer. A detailed description of data collection is given in reference [3]. The iron complexes were prepared as described in the literature [1]. tcne was purified by sublimation through alumina before use.

*Cis-**2a***. ^{1}H NMR acetone-d_6 δ 1.96 [t, 1H, H(2), J 4.6 Hz], 4.52 [d, 1H, H(1), J 5.5 Hz], 4.77 [t, 1H, H(3), J 4.6 Hz], 5.02 [t, 1H, H(6), J 3.4 Hz] + 1/2 of 5.30 [m, 2H, H(5)], 5.70 [d, 1H, H(4), J 3.2 Hz], 7.18 [s, 1H, H(7)] + 1/2 of 7.6 [m, 10H, Ar].

*Trans-**2a***. acetone-d_6 δ 2.36 [t, 1H, H(2), J 4.6 Hz], 4.69 [d, 1H, H(1), J 4.6 Hz], 4.85 [t, 1H, H(3), J 4.1 Hz] + 1/2 of 5.30 [m, 2H, H(6)], 5.45 [t, 1H, H(5), J 4.6 Hz], 5.84 [d, 1H, H(4), J 4.7 Hz], 7.39 [s, 1H, H(7)] + 1/2 of 7.6 [m, 10H, Ar].

3a. acetone d_6 δ 3.95 [t, 1H, H(2), J 2.9 Hz], 4.05 [5, 1H, H(5), J 2.9 Hz], 4.40 [d, 1H, H(5), $J = 3.3$ Hz], 4.85 [m, 1H, H(1)], 6.20 [m, 2H, H(3) + H(4)], 6.80 [2, 1H, H(7)], 7.62 [m, 5H, Ar].

1b. acetone-d_6 δ 3.40 [t, 1H, H(3), J 2.9 Hz], 4.30 [d, 1H, H(5), J 2.4 Hz], 5.7–6.0 [m, 4H, H(1) + H(3) + H(4) + H(5)], 7.4 [m, 10H, Ar].

2b. acetone-d_6 δ 2.39 [t, 1H, H(2), J 3.5 Hz], 4.70 [d, 1H, H(1), J 3.0 Hz], 4.88 [t, 1H, H(3), J 3.0 Hz], 5.16 [t, 1H, H(6), J 3.0 Hz], 5.30 [t, 1H, H(5), J 3.5 Hz], 5.68 [d, 1H, H(4), J 4.0 Hz].

3b. acetone-d_6 δ 4.10 [t, 2H, H(2) + H(5), J 5.4 Hz], 4.58 [d, 2H, H(1) + H(6), J 4.1 Hz], 6.18 [m, 2H, H(3) + H(4)].

References

1 S.K. Chopra, M.J. Hynes, G. Moran, J. Simmie and P. McArdle, Inorg. Chim. Acta, 63 (1982) 177.
2 Z. Goldschmidt and Y. Bakal, J. Organomet. Chem., 179 (1979) 197.
3 S.K. Chopra, D. Cunningham, S. Kavanagh, P. McArdle and G. Moran, J. Chem. Soc., Dalton Trans., in press.
4 G. Moran, Ph.D. Thesis National University of Ireland, 1982.
5 Z. Goldschmidt, H.E. Gottlieb and D. Cohen, J. Organomet. Chem., 294 (1985) 219.
6 Z. Goldschmidt, H.E. Gottlieb, E. Genizi, D. Cohen and I. Goldschmidt, J. Organomet. Chem., 301 (1986) 337.
7 R.B. Woodward and R. Hoffman, The Conservation of Orbital Symmetry, Verlag Chemie, Academic Press, New York, 1970.
8 J.J. Gjewski, Acc. Chem. Res., 13 (1980) 142.
9 T.A. Albright, P. Hoffman and R. Hoffman, J. Amer. Chem. Soc., 99 (1977) 7546.
10 T.A. Albright, P. Hoffmann and R. Hoffmann, Chem. Ber., 111 (1978) 1591.
11 K.J. Karel, T.A. Albright and M. Brookhart, Organometallics, 1 (1982) 419.
12 C.K. Johnson, ORTEP, Oak Ridge Nat. Lab. (Rep.) ORNL (US), 1965-3794, revised 1971.
13 G.M. Sheldrick SHELX, A computer program for crystal structure determination, University of Cambridge, (Cambridge England) 1976.
14 J.A.D. Jeffreys and C. Metters, J. Chem. Soc., Dalton Trans., (1977) 729.
15 R.P. Hodge, J. Amer. Chem. Soc., 86 (1964) 5429.
16 Forticon8 (QCPE 344), J. Howell, A. Ressi, D. Wallace, K. Haraki and R. Hoffman, QCPE, Dept. of Chemistry, Indiana University, Bloomington, Indiana 47405.